CERN-TH.5687/90

On The Threshold Behaviour of Heavy Top Production

V. Fadin
CERN — Geneva
and
Institute for Nuclear Physics
630090 Novosibirsk, USSR

V. Khoze
CERN — Geneva
and
Leningrad Institute for Nuclear Physics
188350 Gatchina, USSR

and
T. Sjöstrand
CERN — Geneva

Abstract:
If the top is heavy, as now seems likely, the $t\bar{t}$ threshold behaviour is given by perturbative QCD. The QCD threshold interaction can be formulated in terms of a potential, attractive or repulsive depending on whether the $t\bar{t}$ is in a colour singlet or octet state. This gives a suppression factor for octet production. Singlet production is enhanced, both above threshold and, by resonance formation, below it. While e^+e^- annihilation only proceeds in the singlet $t\bar{t}$ channel, hadron-hadron collisions contain a non-trivial mixture of the two. In this paper we review the relevant threshold factor formulae, and present phenomenological consequences for hadron colliders, current and future.

CERN-TH.5687/90
March 1990

1 Introduction

We can feel quite confident that the sixth flavour – the top – exists. The best lower mass limit is given by CDF [1], $m_t \geq 89$ GeV at 95% CL (provided that standard semileptonic decays occur at the expected rate). In the framework of the standard model, the recent measurements of m_Z and m_W/m_Z, when combined with neutrino scattering data, suggest [2] a top mass $m_t \simeq 135 \pm 35$ GeV. The observation of large B_d^0–$\overline{B}_d^0$ mixing by ARGUS and CLEO leads to similar conclusions [3], $m_t \simeq 100 - 150$ GeV. To summarize, there exist credible experimental restrictions

$$90 \leq m_t \leq 180 - 200 \text{ GeV}. \tag{1}$$

It is therefore interesting to consider the consequences of a heavy top scenario.

The properties of a heavy top will be in marked contrast to those of charm and bottom. Specifically, for large enough quark mass (roughly $m_t \geq 100$ GeV), the influence of non-perturbative effects is small, and quark dynamics is governed only by electroweak and perturbative QCD effects. This has been discussed in detail in Refs. [4,5,6].

In the threshold region, the behaviour is calculable in terms of a QCD Coulomb-like interaction between the t and $\bar{t}$ at small enough distances, with an effective α_S that is reasonably small. In e^+e^- annihilation, where a $t\bar{t}$ pair is produced in a colour singlet state, this gives a situation closely similar to heavy lepton pair production, with α_{EM} replaced by α_S.

In hadron collisions, a $t\bar{t}$ pair may be produced either in a colour singlet state or in a colour octet one (while only the former is allowed in e^+e^- annihilation). The threshold interaction is then given by two-particle Coulomb-like potentials,

$$V^{(s)}(r) = -\frac{4}{3}\frac{\alpha_S(1/r)}{r} \tag{2}$$

for the colour singlet channel, and

$$V^{(8)}(r) = \frac{1}{6}\frac{\alpha_S(1/r)}{r} \tag{3}$$

for the colour octet one.

While the interaction is repulsive in the octet state, multiple gluon exchange between t and $\bar{t}$ can, for sufficiently long-lived quarks, give bound states in the singlet channel, at a distance scale r of the order of $(\alpha_S m_t)^{-1}$. Thus the set of Coulomb-like bound states is formed below the continuum threshold, see Refs. [7,8]. As we shall see, the interactions also imply significant modifications of the cross-sections above threshold.

As heavier and heavier top masses are considered, the top width increases rapidly [4],

$$\Gamma_t \approx (175 \text{ MeV})\left(\frac{m_t}{m_W}\right)^3 \tag{4}$$

for $m_t > m_W$. Therefore toponium states will be increasingly broad, and eventually (for $m_t \simeq 150$ GeV) merge into a smeared below-threshold 'continuum', when classical bound states do not have the time to form before weak decays.

To our knowledge, the effects of Coulomb rescattering of the non-relativistic particles in QED were first discussed by Sommerfeld [9] and Sakharov [10]. Ref. [10] was devoted specifically to the effects of Coulomb attraction in lepton pair production. QCD Coulomb-like effects for the threshold behaviour in the colour singlet channel were rediscovered by Appelquist and Politzer [11].

A detailed study of threshold behaviour for the process $e^+e^- \to t\bar{t}$ was performed in Ref. [5], and of threshold behaviour for general processes in Ref. [6]. In the current paper, we will review the main results obtained in these publications, and perform a phenomenological study of consequences for heavy flavour production in hadron colliders. The results will be valid for the threshold region. This region could be of interest when special experimental cuts are imposed, but it also affects the total cross-section, since the effective parton luminosities sharply decrease with the pair invariant mass-squared, $\hat{s} = \tau s$, see Refs. [12,13].

It should be emphasized that the results presented in this paper will only be valid for the case of a heavy enough top. Assuming an effective smearing over an energy interval $\Delta E \sim |E|$, $E = \sqrt{\hat{s}} - 2m_t$ being the energy above (or below) top threshold, the region of applicability is roughly

$$m_t\left(E^2 + \Gamma_t^2\right)^{3/2} \gg \langle\frac{\alpha_S}{\pi}F^2\rangle, \tag{5}$$

where $\langle\frac{\alpha_S}{\pi}F^2\rangle \approx 0.012 - 0.018\,(\text{GeV})^4$ is the gluonic vacuum condensate [14]. This condition is fulfilled for any E if $m_t \geq 100$ GeV. In particular, $b\bar{b}$ bound state spacings are not consistent with the formulae we will use in the following.

The essence of eq. (5) stems from the small influence of the long-wave non-perturbative potential $g\overline{E}\cdot\bar{r}$ on the unstable heavy quark energy

$$(g\overline{E}\cdot\bar{r})^2_{\text{char}} \sim \langle\alpha_S F^2\rangle r^2_{\text{char}} \sim \langle\alpha_S F^2\rangle\frac{1}{m_t|E+i\Gamma_t|} \ll |E+i\Gamma_t|^2, \tag{6}$$

where the subscript 'char' denotes the characteristic value. Calculations of the non-perturbative corrections to the Green function $G_{E+i\Gamma_t}(0,0)$ of the $t\bar{t}$ system, performed by O.I. Yakovlev and one of us (VF), confirms this qualitative estimate. For example, at $m_t = 100$ GeV, $\delta(\Im G)/\Im G \leq 10\%$ (where $\Im$ denotes the imaginary part).

2 Threshold Factors — Narrow Width Approximation

The Coulomb and width effects modify drastically the threshold behaviour of the process $e^+e^- \to t\bar{t}$ [5]. (QED radiative corrections, connected with bremsstrahlung off the initial leptons, are also of importance.) Thus, analogously to the QED case [10], for the singlet channel the Coulombic attraction leads to a sharp increase of the total cross-section [15]. In the narrow width approximation, the standard threshold factor

$$\beta_t = \sqrt{1 - \frac{4m_t^2}{\hat{s}}} \tag{7}$$

(with $\hat{s} = s$ for e^+e^- annihilation) in the cross-section is replaced by

$$\beta_t|\Psi^{(s)}(0)|^2. \tag{8}$$

Here the squared wave function at the origin is given by

$$|\Psi^{(s)}(0)|^2 = \frac{X_{(s)}}{1-\exp(-X_{(s)})},\ X_{(s)} = \frac{4}{3}\frac{\pi\alpha_S}{\beta_t}. \tag{9}$$

In the limit $\beta_t \to 0$, the total threshold factor

$$\beta_t |\Psi^{(s)}(0)|^2 \to \frac{4}{3}\pi\alpha_S, \tag{10}$$

i.e., is non-vanishing.

It should be noted that, for $X_{(s)} \gg 1$, eq. (9) is twice as large as the well-known Schwinger [16] one-loop result (near threshold $1 + X_{(s)}/2$).

For the octet channel, the cross-section is decreased due to Coulombic repulsion, see eq. (3) and Ref. [6]. The naive threshold factor β_t is now replaced by

$$\beta_t |\Psi^{(8)}(0)|^2, \tag{11}$$

where

$$|\Psi^{(8)}(0)|^2 = \frac{X_{(8)}}{\exp(X_{(8)}) - 1}, \; X_{(8)} = \frac{1}{6}\frac{\pi\alpha_S}{\beta_t}. \tag{12}$$

A detailed analysis of the one-loop QCD corrections to the cross-section of heavy flavour pair production in hadron-hadron collisions has been performed by Nason et al. in Ref. [17]; see also Refs. [12]. In their formulae, the terms of $\mathcal{O}(\pi\alpha_S/\beta_t)$ coincide with the first terms in the decomposition of eqs. (9) and (12). The latter formulae may therefore be viewed as properly exponentiated versions of the first-order result for the threshold behaviour.

Note that the threshold modification, eqs. (9) and (12), is non-negligible even quite far above the threshold. This in particular applies for the colour singlet channel, where the parameter $X_{(s)}$ is large. The equations will have to be taken with a pinch of salt for large invariant $t\bar{t}$ masses, however. Not only is the derivation based on approximations not valid then, but additionally hard perturbative QCD effects (extra hard gluon emission etc.) have to be taken into account [17]. However, one should remember that the characteristic distances (and therefore arguments of α_S) are different for the hard perturbative contributions ($r_{char} \sim 1/m_t$) and for the Coulombic terms ($r_{char} \sim 1/(m_t\beta_t)$).

For a heavy top, the Coulomb effects in the singlet channel totally determine the formation of low-lying bound $t\bar{t}$ states, since perturbative QCD may be used. However, the contribution of these states to the total $t\bar{t}$ cross-section is rather small, of order α_S^3, and concentrated into a small region, $\Delta E \simeq \alpha_S^2 m_t$, of $t\bar{t}$ invariant masses. For more details, see section 4.

In hadron-hadron collisions, the contributions of the different production mechanisms to the pair invariant mass distribution take the standard forms

$$\begin{aligned}
\frac{d\sigma_{gg}}{d\tau} &= \sigma_{gg\to t\bar{t}}(\hat{s}) \left(\frac{d\mathcal{L}_{gg}}{d\tau}\right), \\
\frac{d\sigma_{q\bar{q}}}{d\tau} &= \sigma_{q\bar{q}\to t\bar{t}}(\hat{s}) \left(\frac{d\mathcal{L}_{q\bar{q}}}{d\tau}\right),
\end{aligned} \tag{13}$$

where the bracketed expressions denote effective parton luminosities.

In the Born approximation, averaging over initial parton polarizations, the cross-sections for the subprocesses $gg \to t\bar{t}$ and $q\bar{q} \to t\bar{t}$ are, near threshold, equal to (see e.g. [17,12,13])

$$\begin{aligned}
\sigma^{(B)(th)}_{gg\to t\bar{t}}(\hat{s}) &= \frac{7}{192}\frac{\pi\alpha_S^2}{m_t^2}\beta_t, \\
\sigma^{(B)(th)}_{q\bar{q}\to t\bar{t}}(\hat{s}) &= \frac{1}{9}\frac{\pi\alpha_S^2}{m_t^2}\beta_t.
\end{aligned} \tag{14}$$

In $q\bar{q}$ collisions, where the process has to go via an intermediate s-channel gluon, $t\bar{t}$ pairs are produced exclusively in the colour octet state, while gg collisions give a mixture of octet and singlet contributions. The ratio of octet to singlet states is given by the ratio of colour factors

$$\frac{(d^{abc}/\sqrt{2})^2}{(\delta^{ab}/\sqrt{3})^2} = \frac{5}{2}. \tag{15}$$

Note that, in the $gg \to t\bar{t}$ process, the $t\bar{t}$ pair has spin-parity $J^P = 0^-$ ($S = 0$, $L = 0$), with incoming gluons having total spin $S_G = 1$ and relative orbital momentum $L_G = 1$.

Evidently, the Coulomb gluon exchanges lead to the enhancement of singlet state production and the suppression of the octet state. Since $t\bar{t}$ pairs are produced at a distance of the order of $1/m_t$, which is much less than the characteristic distance $r_{char} \simeq 1/p_{char} \simeq 1/(m_t\beta_t)$ ($\beta_t \sim \alpha_S$ for bound states), one can use the results of the analysis in Refs. [5,6]. The naive recipe for the singlet part of the cross-section gives

$$\sigma^{(s)}_{gg\to t\bar{t}} = \frac{2}{7}\sigma^{(B)}_{gg\to t\bar{t}} |\Psi^{(s)}(0)|^2. \tag{16}$$

For the octet part one has

$$\begin{aligned}
\sigma^{(8)}_{gg\to t\bar{t}} &= \frac{5}{7}\sigma^{(B)}_{gg\to t\bar{t}} |\Psi^{(8)}(0)|^2, \\
\sigma^{(8)}_{q\bar{q}\to t\bar{t}} &= \sigma^{(B)}_{q\bar{q}\to t\bar{t}} |\Psi^{(8)}(0)|^2.
\end{aligned} \tag{17}$$

3 Threshold Factors — Width Influence

The formulae above do not explicitly take into account the effects of bound states and a non-vanishing Γ_t value. When this is done, one obtains [6]

$$\begin{aligned}
\sigma^{(s)}_{gg\to t\bar{t}} &= \frac{2}{7}\sigma^{(B)}_{gg\to t\bar{t}} \frac{4\pi}{m_t^2\beta_t} \Im G^{(s)}_{E+i\Gamma_t}(0,0), \\
\sigma^{(8)}_{gg\to t\bar{t}} &= \frac{5}{7}\sigma^{(B)}_{gg\to t\bar{t}} \frac{4\pi}{m_t^2\beta_t} \Im G^{(8)}_{E+i\Gamma_t}(0,0), \\
\sigma^{(8)}_{q\bar{q}\to t\bar{t}} &= \sigma^{(B)}_{q\bar{q}\to t\bar{t}} \frac{4\pi}{m_t^2\beta_t} \Im G^{(8)}_{E+i\Gamma_t}(0,0).
\end{aligned} \tag{18}$$

Here E is the energy above or below threshold, $E = \sqrt{\hat{s}} - 2m_t$, Γ_t is the top weak decay width, eq. (4), $G^{(s,8)}_{E+i\Gamma_t}(\bar{r},\bar{r}')$ is the Green function of the $t\bar{t}$ system in the colour singlet or octet state, respectively, and $\Im G$ its imaginary part [5,6]

$$\begin{aligned}
\Im G^{(s)}_{E+i\Gamma_t}(0,0) &= \frac{m_t^2}{4\pi}\left[\frac{p_2}{m_t} + \frac{2p_s}{m_t}\arctan\frac{p_2}{p_1} + \right. \\
&\quad \left. + \frac{2p_s^2}{m_t^2}\sum_{n=1}^{\infty}\frac{1}{n^4}\frac{\Gamma_t p_s n + p_2(n^2\sqrt{E^2+\Gamma_t^2} + p_s^2/m_t)}{(E + p_s^2/(m_t n^2))^2 + \Gamma_t^2}\right], \\
\Im G^{(8)}_{E+i\Gamma_t}(0,0) &= \frac{m_t^2}{4\pi}\left[\frac{p_2}{m_t} + \frac{2p_8}{m_t}\arctan\frac{p_2}{p_1} + \frac{2p_8^2}{m_t^2}\sum_{n=1}^{\infty}\frac{m_t p_2}{(np_1 - p_8)^2 + n^2p_2^2}\right],
\end{aligned} \tag{19}$$

where

$$p_s = \frac{2}{3}m_t\alpha_S.$$

$$p_8 = -\frac{1}{12} m_t \alpha_S, \tag{20}$$
$$p_{1,2} = \left[\frac{m_t}{2} \left(\sqrt{E^2 + \Gamma_t^2} \mp E \right) \right]^{1/2}.$$

The $\Im G^{(s)}$ and $\Im G^{(8)}$ are not unrelated but, in fact, $\Im G^{(8)}$ may be obtained from $\Im G^{(s)}$ by the substitution $p_s \to p_8$. The $\Im G^{(8)}$ formula presented here contains an additional trivial rewrite, where the spurious singularities for $E = -p_8^2/(m_t n^2) \pm i\Gamma_t$ have been removed (both the numerator and the denominator of one term in the series vanish at each of these points, but the ratio is finite).

In the singlet channel, the series includes the contribution from an infinite set of bound states, at energies $E_n = -p_s^2/(m_t n^2) = -4m_t \alpha_S^2/(9n^2)$, with total integrated contributions $\propto 1/n^3$, and with a common width $2\Gamma_t$ given entirely by weak decays.

The formulae above do not take into account the energy dependence of the top self-energy graphs of the kind $t \to b + W^+ \to t$, and so would break down for m_t too close to $m_b + m_W$.

In section 5, we will compare the naive expression with the full one.

4 Bound State Formation

If the $t\bar{t}$ pairs in the $gg \to t\bar{t}$ process are produced in the colour singlet state, they can create bound states T with spin-parity $I^P = 0^-$. Combining eqs. (13) and (18), the total cross-section for this mechanism may be written as

$$\begin{aligned} \sigma_{gg \to T} &= \int_{\tau_0}^{4m_t^2/s} \sigma^{(s)}_{gg \to t\bar{t}}(\hat{s}) \left(\frac{d\mathcal{L}_{gg}}{d\tau} \right) d\tau \\ &= \int_{\tau_0}^{4m_t^2/s} \frac{2}{7} \sigma^{(B)}_{gg \to t\bar{t}}(\hat{s}) \frac{4\pi}{m_t^2 \beta_t} \Im G^{(s)}_{E+i\Gamma_t}(0,0) \left(\frac{d\mathcal{L}_{gg}}{d\tau} \right) d\tau. \end{aligned} \tag{21}$$

Here $\tau_0 \simeq 4(m_b + m_W)^2/s$ is an effective lower cut-off, below which the cross-section is assumed to be negligible. This cut-off cannot be read off directly from the $\Im G^{(s)}$ expression in eq. (19), since the width Γ_t is assumed to be energy-independent in that equation. In a more complete description, this width is indeed $\hat{s}$-dependent, with a sharp change when $t \to b + W$ decays are no longer allowed for on-mass-shell W particles.

One can obtain a simple approximate expression for the bound state total cross-section if one uses eq. (19) in the limit of $\Gamma_t \to 0$. Then, for $E < 0$,

$$\Im G^{(s)}_{E+i\Gamma_t} \to \sum_{n=1}^{\infty} \frac{p_s^3}{n^3} \delta\left(E + \frac{p_s^2}{m_t n^2} \right). \tag{22}$$

If the variation of the effective luminosity $d\mathcal{L}_{gg}/d\tau$ is neglected in the range $(4m_t^2/s)(1 - p_s^2/2m_t^2)^2 \leq \tau \leq 4m_t^2/s$, one obtains

$$\sigma_{gg \to T} \approx \left(\frac{d\mathcal{L}_{gg}(4m_t^2/s)}{d\tau} \right) \frac{\pi^2 \alpha_S^2}{6s} \left(\frac{p_s}{m_t} \right)^3 \zeta(3), \tag{23}$$

where ζ is the Riemann zeta function, $\zeta(3) = \sum_{n=1}^{\infty} n^{-3} \approx 1.2$.

Note that bound states can also be created via the 'bremsstrahlung process', $q\bar{q} \to (t\bar{t})g$, shown in Fig. 1. Here the emission of an additional gluon transforms the (originally colour octet) $t\bar{t}$ pair into a colour singlet state. Since the effective gluon-gluon luminosity decreases

much more rapidly than the quark-antiquark one (in a $p\bar{p}$ collider) when τ tends to unity, the contribution of this mode could be important when the total energy of the colliding hadrons is near the threshold of $t\bar{t}$ production.

The Born level cross-section for the emission of a gluon, with the remainder $t\bar{t}$ system in a colour singlet state, can be easily obtained using the results of [18]:

$$\frac{d\sigma^{(s)(B)}_{q\bar{q} \to (t\bar{t})g}}{d\hat{s}'} = \frac{1}{27} \frac{4}{3} \alpha_S^3 \frac{\hat{s} - 4m_t^2}{\hat{s}^3} \beta_t'. \tag{24}$$

Here $\hat{s}$ and $\hat{s}'$ are the $t\bar{t}$ invariant mass-squared before and after the final state gluon emission, respectively, and $\beta_t' = \sqrt{1 - 4m_t^2/\hat{s}'}$.

The Coulomb and width effects modify the Born cross-section in a manner similar to eq. (18),

$$\frac{d\sigma^{(s)}_{q\bar{q} \to (t\bar{t})g}}{d\hat{s}'} = \frac{1}{27} \frac{4}{3} \alpha_S^3 \frac{\hat{s} - 4m_t^2}{\hat{s}^3} \frac{4\pi}{m_t^2} \Im G^{(s)}_{E'+i\Gamma_t}(0,0), \tag{25}$$

where $E' = \sqrt{\hat{s}'} - 2m_t$.

The total 'bremsstrahlung mechanism' cross-section for bound state production can be obtained by integration:

$$\sigma_{q\bar{q} \to Tg} = \int_{4m_t^2/s}^{1} d\tau \left(\frac{d\mathcal{L}_{q\bar{q}}}{d\tau} \right) \int_{s\tau_0}^{4m_t^2} d\hat{s}' \frac{d\sigma^{(s)}_{q\bar{q} \to (t\bar{t})g}}{d\hat{s}'}, \tag{26}$$

where the lower effective cut-off $s\tau_0 = 4(m_b + m_W)^2$.

In the limit that Γ_t tends to zero, eq. (22) may be used to derive the approximate expression

$$\sigma_{q\bar{q} \to Tg} = \int_{4m_t^2/s}^{1} d\tau \left(\frac{d\mathcal{L}_{q\bar{q}}}{d\tau} \right) \frac{\pi \alpha_S^3 (s\tau - 4m_t^2)}{3s^3 \tau^3 m_t} \left(\frac{4p_s}{3} \right)^3 \zeta(3). \tag{27}$$

It is worthwhile to note that a 'bremsstrahlung process' analogous to the one discussed above should be the main source of $t\bar{t}$ bound state formation in lepton-hadron collisions. Here the $t\bar{t}$ pair is produced by gluon (g) and electroweak boson (γ/Z^0) fusion, and again the emission of an additional gluon is necessary to transform the $t\bar{t}$ pair into a colour singlet state. The resulting 'bremsstrahlung mechanism' cross-section for bound state production could be obtained in a way analogous to the one above for hadron colliders.

5 Results

In the following, we will study the implications of the threshold modifications introduced above. For the calculations, the EHLQ set 1 structure functions [13], with $\Lambda = 200$ MeV, have been used throughout. Although the absolute results would be somewhat different with another choice, none of the qualitative features would be affected. For Monte Carlo integration, the PYTHIA program [19] has been used, with the full $q\bar{q} \to t\bar{t}$ and $gg \to t\bar{t}$ Born cross-sections (rather than the approximate ones in eq. (14)).

Normally, a running α_S is used, with an argument corresponding to the simplest dependence on the characteristic virtuality in the process, $Q^2 = \bar{p}_Q^2 \simeq m_t \sqrt{E^2 + \Gamma_t^2}$, i.e.,

$$\alpha_S = \frac{12\pi}{23 \ln(m_t \sqrt{E^2 + \Gamma_t^2}/\Lambda^2)}, \tag{28}$$

with $\Lambda = 200$ MeV. When using fixed α_S values, these were chosen to agree with the running α_S value at the first maximum of the cross-section (the lowest bound state).

Fig. 2 shows the importance of the enhancement and suppression factors in eqs. (9) and (12). Note that, due to $X_{(1)}$ being much larger than $X_{(8)}$, the singlet enhancement factor deviates more from unity than the octet suppression factor does, and that therefore there is a net increase in the gg channel.

Figure 3 illustrates the threshold behaviour in the colour singlet channel for various values of the top mass, $m_t = 100$, 140 and 200 GeV. Even for 100 GeV, only the lowest bound state shows up as an explicit peak in the cross-section, while all the rest merge into a broad bump. At 200 GeV the $t\bar{t}$ levels completely overlap, and the resonance structure is practically washed out and buried in the continuum [4,5,6].

One should note that the curves above do not include any experimental smearing effects. Unlike the case of J/Ψ, Υ, where decays into an e^+e^- or $\mu^+\mu^-$ pair give a characteristic signal with good mass resolution, toponium formation would not be distinguishable from continuum $t\bar{t}$ production, with its well-known bad mass resolution. In hadron colliders, it would therefore be impossible to study the details of the threshold behaviour, even for $m_t = 100$ GeV. An e^+e^- experiment, where one would just have to consider the variation of the total hadronic cross-section with energy, could in principle do better, but here also effects of beam energy spread and initial state photon radiation would tend to obscure the theoretical picture.

Above threshold, the simple enhancement factor formula, eq. (9), agrees well with the full answer involving $\Im G_{E+i\Gamma_t}(0,0)$, but the simple answer does not include the effect of bound state formation below threshold. On the other hand, $\Im G_{E+i\Gamma_t}(0,0)$ is derived specifically with respect to threshold behaviour, and the formula breaks down far away from the threshold region. Specifically, the first term in eq. (19) is proportional to $\sqrt{E}$, and will give an unphysical asymptotic behaviour.

The corresponding threshold behaviour in the colour octet channel is displayed in Fig. 4. While the narrow width approximation result gives a suppression compared to the naive β factor everywhere, the full expression gives an enhancement close to (and below) threshold, simply due to the possibility of a top quark being lighter than its nominal width. Again we note the onset of the bad high energy behaviour of the full $\Im G_{E+i\Gamma_t}(0,0)$ expression for $E \geq 15GeV$.

Figures 2–4 illustrate the threshold modifications arising from Coulomb effects. In Fig. 5 consequences are shown for current and future hadron colliders, in terms of the cross-section as a function of the $t\bar{t}$ invariant mass. Monte Carlo results are for 10,000 events at each energy, and have been obtained by a sampling of the correct Born term expression, multiplied by the relevant modification factors.

At 630 GeV, where the $q\bar{q}$ mechanism dominates, the total cross-section is reduced by about 10%. As the energy is increased, the gg channel becomes the more important one, and so the total cross-section is increased by Coulomb effects. At LHC and SSC the increase is roughly 10%. The crossover is at around TeV energies, see Fig. 6. The shape of the invariant mass distribution is also changed somewhat by the introduction of threshold factors, not unexpectedly with the effect most marked close to threshold.

Note that the *analytical* expressions for the cross-sections of the processes $q\bar{q} \to t\bar{t}$ and $gg \to t\bar{t}$ in the threshold region change drastically. The lack of a large *numerical* difference in the total hadron-hadron production cross-section is connected, on the one hand, with the relatively small colour factor 2/7 for the singlet channel, and, on the other hand, with the

smallness of the damping parameter $X_{(8)}$ for the dominant octet channel. Further, in hadron collisions, the integration over a large range of $t\bar{t}$ masses and summation over contributing structure functions reduce the observable Coulomb effects.

In Fig. 6 the cross-section for bound state toponium is also shown. Over the energy range considered, the $gg \to T$ rate is everywhere more than two orders of magnitude below the total top continuum cross-section. The process $q\bar{q} \to Tg$ is even further suppressed, by something like four orders of magnitude compared to the $q\bar{q} \to t\bar{t}$ continuum process. Of the two processes for T bound state formation, the latter will only win over the former for top quark masses so close to the threshold of the machine that cross-sections are unobservably small anyway. Of course, bound state formation is still of importance for an understanding of the differential cross-section behaviour close to threshold.

6 Summary

Let us emphasize that our purpose here was not the detailed description of all QCD corrections, but the demonstration of the Coulombic $\pi\alpha_S/\beta$ effects, in differential and total cross-sections. The reader can find a comprehensive analysis of the one-loop QCD corrections to the heavy quark pair production in [17,12]. The two approaches are complementary. One aspect not included in the one-loop formulae, but included here, is bound state production. The one-loop approach will still very likely be reasonably good in a dual sense, i.e. in giving the total cross-section near to threshold, even if not the detailed shape.

The threshold modifications are especially important for e^+e^- annihilation. This process is entirely colour singlet, and a significant enhancement of the cross-section is therefore to be expected. It is important to take this into account, e.g. for the determination of the top quark mass, once a signal is seen. We also mention that, for $m_t \leq 100$ GeV, one may hope to extract information on $\alpha_S(k_n)$, by a comparison of cross-sections in the lowest resonance states (here $k_n = (2/3)\alpha_S(k_n)m_t$ is the momentum of the relative t and $\bar{t}$ motion in the n^{th} Coulombic state).

For hadron colliders, effects are not as spectacular. In particular, the total top cross-section is only changed by 10% at most over a wide range of CM energies. As irony has it, the effect is actually one of decreasing the cross-section at lower energies; i.e. it does not make top searches any easier at current machines. Once the top is found, the correction factors studied here will again be of relevance for mass determinations. In particular, at all CM energies, there is a net enhancement very close to the threshold, due to the removal of the β_t phase space factor for 2/7 of the $gg \to t\bar{t}$ cross-section.

Acknowledgements

The authors are indebted to Yu. L. Dokshitzer, R. K. Ellis, J. H. Kühn, A. Martin, A. H. Mueller, P. Nason, A. D. Sakharov†, E. V. Shuryak, M. B. Voloshin, and P. M. Zerwas for useful discussions. Two of us (VF and VK) are very much indebted to the CERN theory division for the hospitality during our visits.

References

[1] CDF Collaboration, F. Abe *et. al.*, Phys. Rev. Lett. **64** (1990) 142;
CDF Collaboration, K. Sliwa, talk at the Moriond meeting, Les Arcs, March 11 - 17, 1990

[2] J. Ellis, G. L. Fogli, Phys. Lett. **B231** (1989) 189
P. Langacker, Phys. Rev. Lett. **63** (1989) 1920
D. Haidt, contribution to the EPS Conference, Madrid (1989)

[3] H. Schröder, *in* ed. R. Kotthaus, J. Kühn, Proceedings of the 24^{th} International Conference on High Energy Physics (Springer-Verlag, Berlin, 1989), p. 73, and references therein

[4] I. Bigi, Yu. Dokshitzer, V. Khoze, J. Kühn, P. Zerwas, Phys. Lett. **B181** (1986) 157

[5] V. Fadin, V. Khoze, JETP Lett. **46** (1987) 417; Yad. Fiz. **48** (1988) 487

[6] V. Fadin, V. Khoze, *in* Proceedings of the 24^{th} Winter School of the LNPI (Leningrad, 1989), vol. I, p. 3

[7] M. Voloshin, Nucl. Phys. **B154** (1979) 365; Yad. Fiz. **36** (1982) 247

[8] H. Leutwyler, Phys. Lett. **98B** (1981) 447

[9] A. Sommerfeld, 'Atombau und Spektrallinien', Bd. 2 (Vieweg, Braunschweig, 1939)

[10] A. D. Sakharov, JETP **18** (1948) 631

[11] T. Appelquist, H. D. Politzer, Phys. Rev. Lett. **34** (1975) 43; Phys. Rev. **D12** (1975) 1404

[12] W. Beenakker, H. Kuijf, W. L. van Neerven, J. Smith, Phys. Rev. **D40** (1989) 54;
R. J. N. Phillips, Rutherford preprint RAL-89-036 (1989)

[13] E. Eichten, I. Hinchliffe, K. Lane, C. Quigg, Rev. Mod. Phys. **56** (1984) 579; **58** (1986) 1065

[14] A. I. Vainshtein, V. I. Zakharov, M. A. Shifman, JETP Lett. **27** (1978) 60
M. B. Voloshin, Yu. M. Zaitsev, Uspekhi Fiz. Nauk **152** (1987) 361

[15] S. Güsken, J. H. Kühn, P.M. Zerwas, Phys. Lett. **155B** (1985) 185

[16] J. Schwinger, 'Particles, Sources, and Fields', Vol. 2 (Addison-Wesley, Reading, Mass., 1970)

[17] P. Nason, S. Dawson, R. K. Ellis, Nucl. Phys. **B303** (1988) 607

[18] V. N. Baier, V. A. Khoze, Zh. Eksper. Teor. Fiz. **48** (1965) 946

[19] H.-U. Bengtsson, T. Sjöstrand, Computer Physics Commun. **46** (1987) 43

Figure Captions

Fig. 1 Formation of a bound state by final state gluon emission.

Fig. 2 Threshold behaviour for $m_t = 100$ GeV and fixed $\alpha_S = 0.196$. Full line is the standard threshold factor β_t, the dashed one is the enhanced singlet channel factor $\beta_t|\Psi^{(1)}(0)|^2$, and the dash-dotted one the suppressed octet channel factor $\beta_t|\Psi^{(8)}(0)|^2$. The dotted one gives the combination relevant for the gg channel, 2/7 singlet and 5/7 octet. E is energy above nominal top threshold at $2m_t$.

Fig. 3 Threshold behaviour for colour singlet channel, with running α_S. The full line is standard threshold factor β_t, the dashed one the naive enhancement recipe $\beta_t|\Psi^{(1)}(0)|^2$, and the dash-dotted one the expression $4\pi\Im G^{(1)}_{E+i\Gamma_t}(0,0)/m_t^2$. Note the change in vertical scale between a), b) and c).
a) $m_t = 100$ GeV.
b) $m_t = 140$ GeV.
c) $m_t = 200$ GeV.

Fig. 4 Threshold behaviour for colour octet channel, with running α_S. The full line is standard threshold factor β_t, the dashed one the naive suppression recipe $\beta_t|\Psi^{(8)}(0)|^2$, and the dash-dotted one the expression $4\pi\Im G^{(8)}_{E+i\Gamma_t}(0,0)/m_t^2$.
a) $m_t = 100$ GeV.
b) $m_t = 140$ GeV.
c) $m_t = 200$ GeV.

Fig. 5 Invariant mass distribution of $t\bar{t}$ pairs for $m_t = 100$ GeV. Full line is without any Coulomb corrections, dashed and dotted ones with corrections, using a fixed or running α_S, respectively. Contribution below threshold is not included.
a) For the $Sp\bar{p}S$ collider at 630 GeV.
b) For the $TeVI$ collider at 1.8 TeV.
c) For the LHC collider at 15 TeV.
d) For the SSC collider at 40 TeV.

Fig. 6 The energy dependence of the total cross-section for $t\bar{t}$ production, subdivided into contributions from $q\bar{q} \to t\bar{t}$ (full), $gg \to t\bar{t}$ continuum (dashed), $gg \to t\bar{t}$ bound state (dash-dotted), and $q\bar{q} \to g(t\bar{t})$ bound state (dotted). Results are for $m_t = 100$ GeV and running α_S.

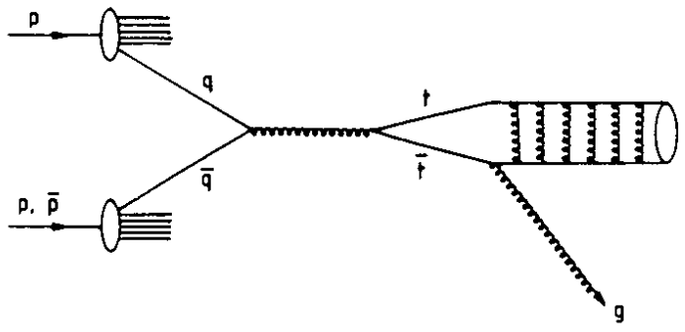

Fig. 1

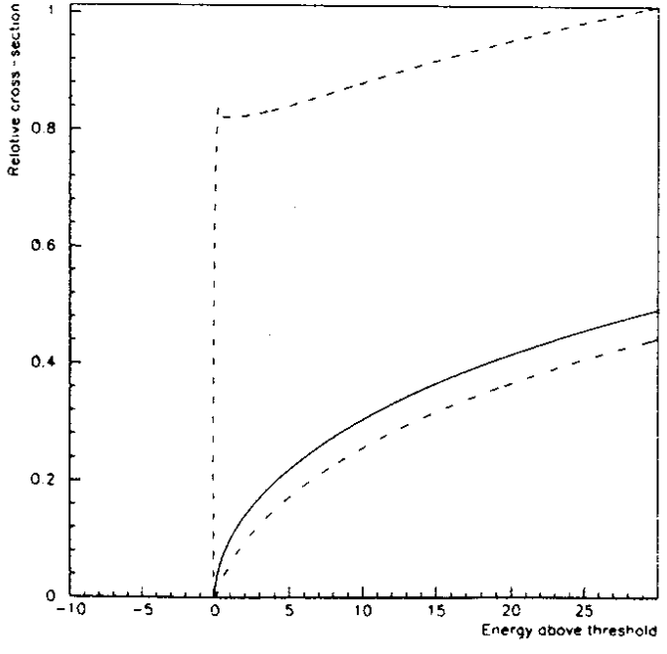

Fig. 2

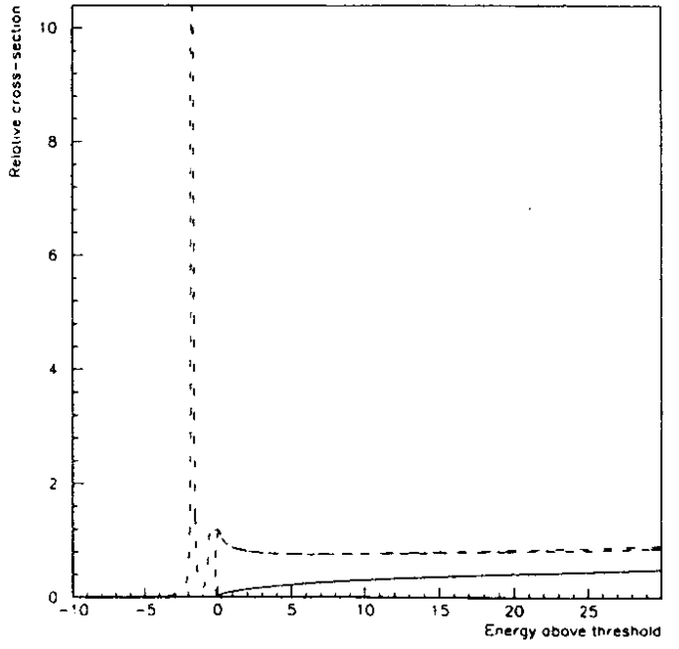

Fig. 3a

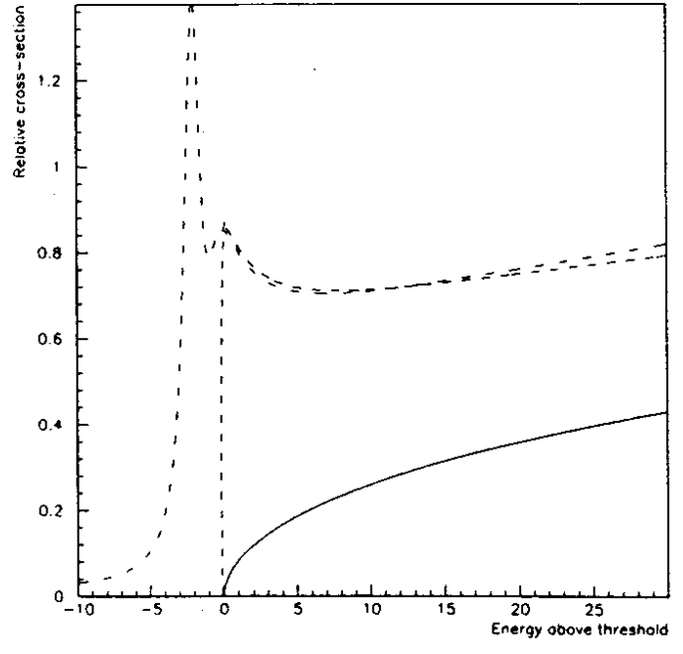

Fig. 3b

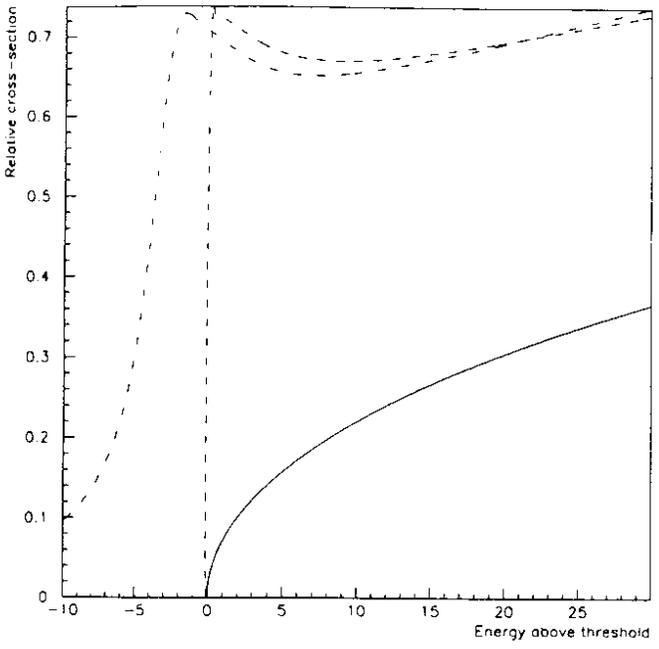

Fig. 3c

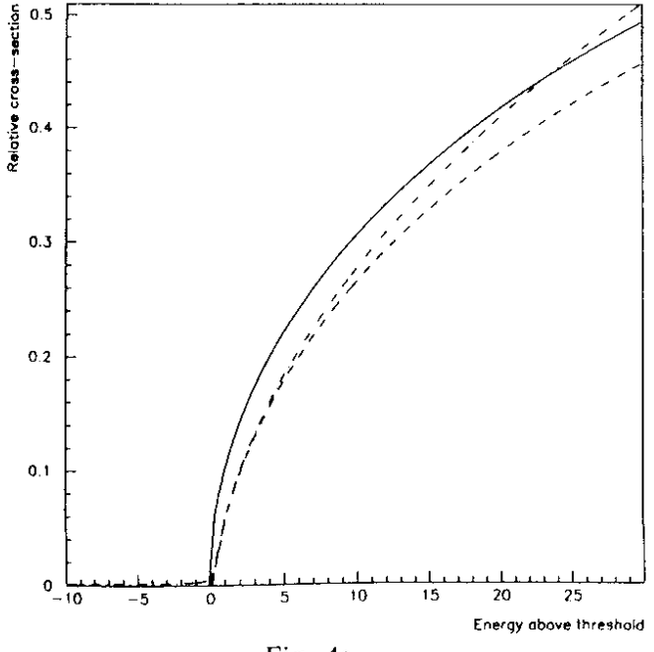

Fig. 4a

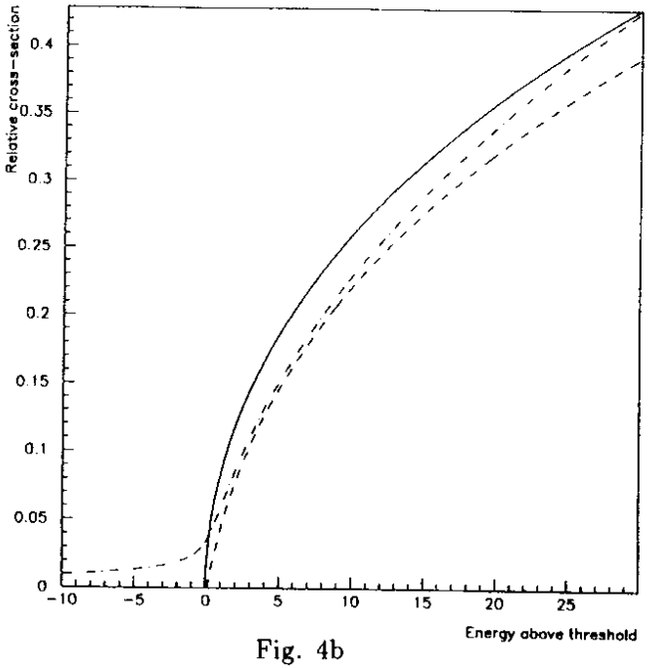

Fig. 4b

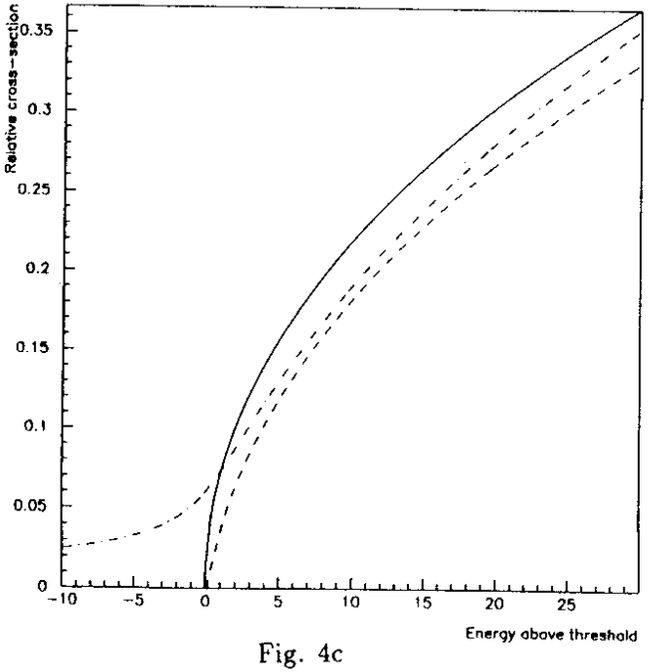

Fig. 4c

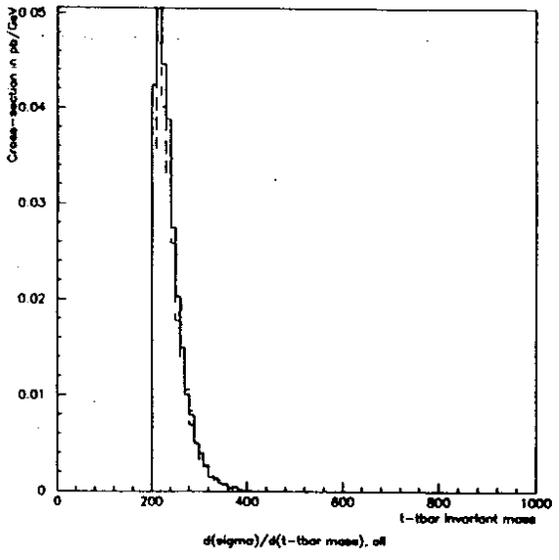

Fig. 5a

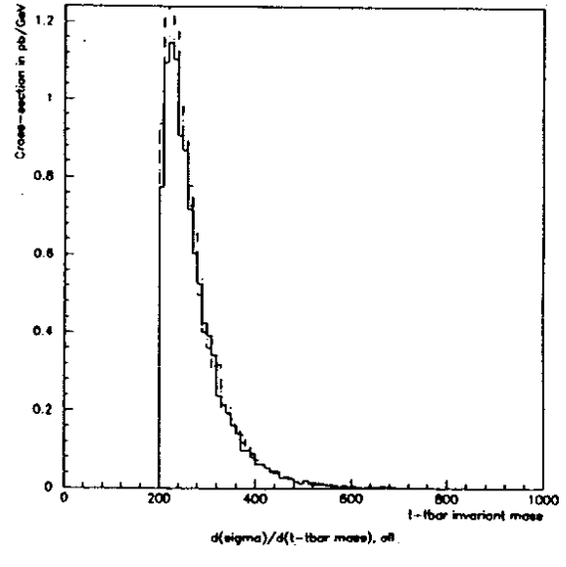

Fig. 5b

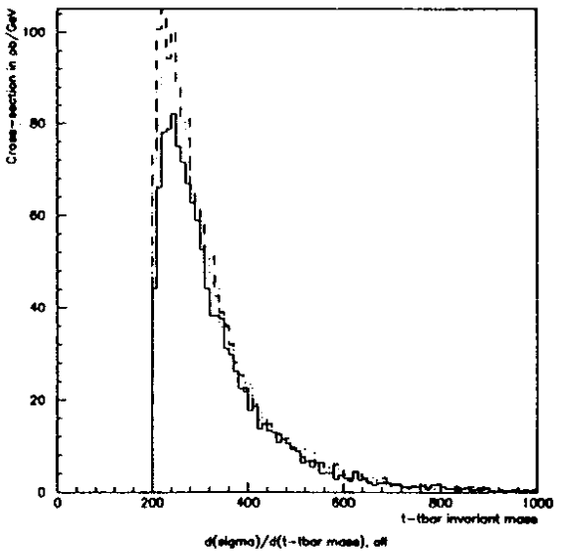

Fig. 5c

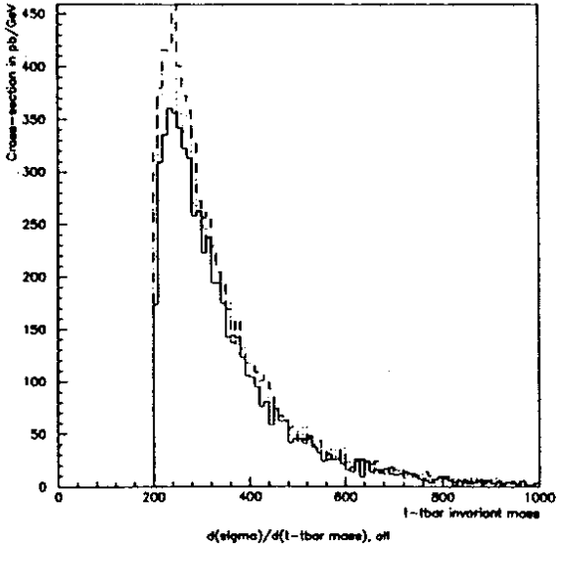

Fig. 5d

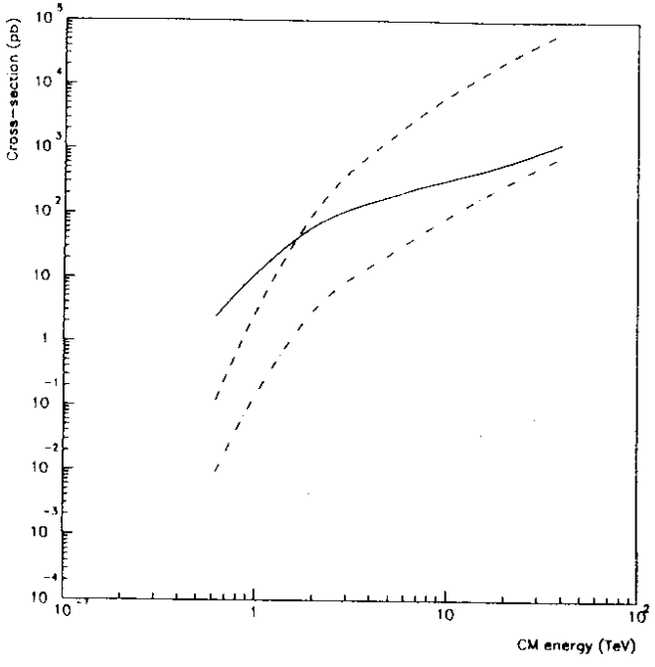

Fig. 6